

Research



Cite this article: Martin BT, Dudley PN, Kashef NS, Stafford DM, Reeder WJ, Tonina D, Del Rio AM, Scott Foott J, Danner EM. 2020 The biophysical basis of thermal tolerance in fish eggs. *Proc. R. Soc. B* **287**: 20201550. <http://dx.doi.org/10.1098/rspb.2020.1550>

Received: 30 June 2020

Accepted: 28 September 2020

Subject Category:

Ecology

Subject Areas:

ecology

Keywords:

thermal tolerance, oxygen limitation, temperature, egg, embryo, metabolic rate

Author for correspondence:

Benjamin T. Martin

e-mail: b.t.martin@uva.nl

Electronic supplementary material is available online at <https://doi.org/10.6084/m9.figshare.c.5170545>.

The biophysical basis of thermal tolerance in fish eggs

Benjamin T. Martin^{1,2,3}, Peter N. Dudley^{2,3}, Neosha S. Kashef^{2,3}, David M. Stafford^{2,3}, William J. Reeder⁴, Daniele Tonina⁴, Annelise M. Del Rio⁵, J. Scott Foott⁶ and Eric M. Danner^{2,3}

¹Institute for Biodiversity and Ecosystem Dynamics, University of Amsterdam, Amsterdam, The Netherlands

²Institute of Marine Science, University of California Santa Cruz, USA

³Southwest Fisheries Science Center, National Marine Fisheries Service, National Oceanic Atmospheric Administration, La Jolla, CA, USA

⁴Center for Ecohydraulics Research, University of Idaho, Boise, ID, USA

⁵Department of Animal Science, University of California Davis, Davis, CA, USA

⁶U.S. Fish and Wildlife Service, CA-NV Fish Health Center, Anderson, CA, USA

BTM, 0000-0003-3927-0449; EMD, 0000-0003-0860-2869

A warming climate poses a fundamental problem for embryos that develop within eggs because their demand for oxygen (O₂) increases much more rapidly with temperature than their capacity for supply, which is constrained by diffusion across the egg surface. Thus, as temperatures rise, eggs may experience O₂ limitation due to an imbalance between O₂ supply and demand. Here, we formulate a mathematical model of O₂ limitation and experimentally test whether this mechanism underlies the upper thermal tolerance in large aquatic eggs. Using Chinook salmon (*Oncorhynchus tshawytscha*) as a model system, we show that the thermal tolerance of eggs varies systematically with features of the organism and environment. Importantly, this variation can be precisely predicted by the degree to which these features shift the balance between O₂ supply and demand. Equipped with this mechanistic understanding, we predict and experimentally confirm that the thermal tolerance of these embryos in their natural habitat is substantially lower than expected from laboratory experiments performed under normoxia. More broadly, our biophysical model of O₂ limitation provides a mechanistic explanation for the elevated thermal sensitivity of fish embryos relative to other life stages, global patterns in egg size and the extreme fecundity of large teleosts.

1. Introduction

Predicting how animal populations will respond to a warming planet is among the most pressing challenges in ecology. Like many animals, fish transition through several life stages, which can differ substantially in their tolerance for elevated temperatures [1–4]. How species respond to climate change will be largely determined by the most sensitive life stages [5]. In addition to the spawning adults, embryos are the most sensitive life stage in fishes, with thermal tolerances on average 8°C lower than other life stages [5]. Thus, the key to predicting how fish populations will respond to climate change is first understanding the mechanisms of thermal tolerance in embryos.

What mechanisms can explain the low thermal tolerance of fish embryos? Unlike other life stages, fish embryos, which develop within eggs, are unable to regulate their supply of O₂ actively through ventilation and must rely on O₂ diffusion across an egg surface [6,7]. The implications of this constraint for O₂ limitation are simple but profound: across species, the metabolic rate of embryos increases in proportion to egg volume [8], but supply occurs across a surface that scales with volume to the two-thirds power; thus larger eggs demand more O₂, but meeting these demands becomes more and more challenging with increasing size. Fish eggs, among the largest aquatic eggs, approach

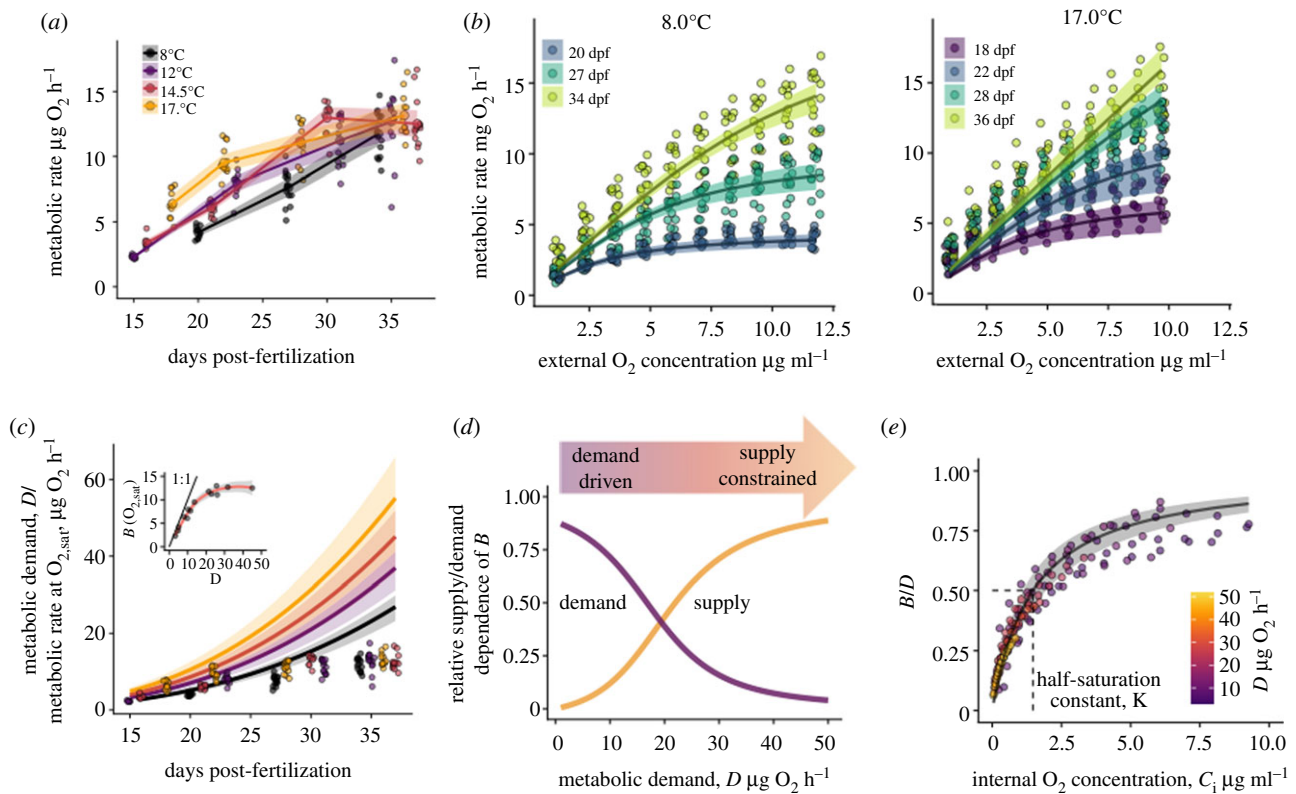


Figure 1. Measuring and modelling O_2 supply and demand in developing salmon embryos (a) Measured metabolic rates of salmon embryos at O_2 saturation depended on development stage and temperature: replicate eggs (small circles), treatment means (large circles, lines) and 95% CI (bands). (b) Observed metabolic rates of individual eggs (circles) as a function of O_2 in the respirometry chamber at intervals of 10% saturation. The developmental stages of experimental embryos (days post-fertilization) are denoted by colour. Lines represent predictions of the biophysical model (95% CI: bands). The two panels show data from the highest and lowest experimental temperatures; data for all experimental temperatures are shown in electronic supplementary material, figure S1 (c) The estimated metabolic demand, D , of embryos increases rapidly with temperature and development day (lines; bands depict 95% CI), while the observed metabolic rate in normoxia plateaus (points, same data as panel (a)). Inset shows the measured realized metabolic at saturated O_2 as a function of the estimated demand. Points represent treatment means for each temperature development day combination ($n = 15$). (d) As the metabolic demand of embryos increases their metabolism switches from being demand driven to supply constrained. Shown is the relative dependence of realized metabolic rate, B , on metabolic demand, D , and supply, C_o , as a function of D , in normoxia; 0 and 1 denote complete independence and proportional dependence respectively (see electronic supplementary material, appendix A1 for calculation). (e) Mean observed metabolic rates, B , scaled by D , across all temperatures, development stages and external O_2 concentrations (points), collapse to a single Michaelis–Menten relationship a function of the within-egg O_2 concentration. Line shows the model-predicted Michaelis–Menten relationship (bands: 95% CI). (Online version in colour.)

sizes where O_2 supply is precariously balanced with demand [8]. Because the metabolic rate of embryos increases exponentially with temperature [9], elevated water temperatures can disrupt this balance and cause O_2 limitation, as metabolic demands rise while supply remains fixed. This suggests a mechanistic basis for the thermal tolerance of fish eggs, where the upper thermal tolerance of eggs is set by a temperature-dependent imbalance between O_2 supply and demand. This hypothesis holds that rather than being a fixed trait, thermal tolerance varies with factors that affect O_2 supply and demand, and that this variation can be predicted from biophysical theory.

Here, we combine mathematical models of O_2 supply and demand with a series of experiments to test whether O_2 limitation sets thermal tolerance in the large aquatic eggs of Chinook salmon (*Oncorhynchus tshawytscha*). By experimentally manipulating both O_2 supply and demand during exposure to a range of temperatures, we demonstrate that the survival of these eggs depends in predictable ways on factors that shift the balance between O_2 supply and demand. Finally, we show how this mechanistic understanding of thermal tolerance can be harnessed to predict the survival of eggs in the complex natural environments in

which they occur in nature: as clusters of eggs buried in gravel beds of streams and rivers. These findings provide a mechanistic explanation for a recent near-complete cohort loss of an endangered salmon population, which occurred at water temperatures much lower than previously thought to be lethal for salmon eggs [8].

2. Results

To test the hypothesis that O_2 limitation underlies the thermal tolerance of fish embryos, we designed a series of respirometry experiments to quantify how O_2 limitation depends on features of the embryo and environment. We then tested whether the degree of O_2 limitation could predict survival of developing embryos across a range of temperatures where both O_2 supply and demand were experimentally manipulated.

To quantify O_2 demand as a function of developmental stage, temperature and ambient O_2 concentration, we conducted a series of closed-system respirometry trials. At early developmental stages, metabolic rate increased with temperature as expected, with roughly a doubling of metabolic rate between 8 to 17°C (figure 1a). However, at

later developmental stages, metabolic rates across treatments plateaued at approximately $15 \mu\text{g O}_2 \text{ h}^{-1}$ at saturation. Additionally, the shape of the function relating metabolic rate to external O_2 concentration varied between early and late development stages. In early development, when the metabolic rate was low, the metabolic rate of eggs was largely independent of ambient O_2 until it was reduced to low concentrations within the respirometry chambers (figure 1*b*; electronic supplementary material, figure S1). While at later developmental stages, metabolic rate was strongly dependent on O_2 concentration, even in normoxia. These two pieces of evidence suggest that salmon embryos late in development are O_2 limited in normoxia even at relatively low temperatures. To test this hypothesis more explicitly, and to quantify O_2 limitation as a function of internal and external states, we developed a mathematical model of O_2 supply and demand.

(a) Model development

We assume that the metabolic rate of an embryo depends both on its intrinsic metabolic demand, D ($\mu\text{g O}_2 \text{ h}^{-1}$), and the availability of O_2 within the egg, C_i ($\mu\text{g O}_2 \text{ ml}^{-1}$). We define D as the metabolic rate of the embryo in the absence of O_2 limitation. During embryonic development, the live tissue mass of salmon embryos increases rapidly as they synthesize new body mass from yolk. As these embryos grow, their metabolic demand increases in proportion to their live tissue mass [10]. Additionally, as in nearly all ectotherms, metabolic rate increases exponentially with temperature [8,9]. Thus, we assume that the metabolic demand of an embryo is

$$D = b_0 M e^{b_1 T}, \quad (2.1)$$

where b_0 and b_1 are parameters that describe the mass, M (mg), and temperature, T (Celsius), the dependence of O_2 demand.

Temperature and mass determine metabolic demand; however, the realized metabolic rate of an embryo also depends on the availability of O_2 within the egg. We assume that like most biological reactions, the rate of metabolism is largely independent of O_2 at high concentrations and determined only by the intrinsic metabolic rate, D , but becomes O_2 limited at low internal O_2 concentrations. We therefore assume the realized metabolic rate, B , is described by a Michaelis–Menten equation,

$$B(M, T, C_i) = \frac{C_i}{K + C_i} D(M, T), \quad (2.2)$$

where K ($\mu\text{g O}_2 \text{ ml}^{-1}$) is the half-saturation constant.

The internal concentration of O_2 is driven by the balance between the depletion of O_2 through metabolism, and the influx of O_2 through diffusion across the egg membrane,

$$\frac{dC_i}{dt} = \frac{I - B}{V_{\text{egg}}}, \quad (2.3)$$

where following Fick's law, the influx of O_2 through the egg, I , is proportional to the concentration gradient at the egg's surface, C_s :

$$I = G(C_s - C_i), \quad (2.4)$$

where, G ($\mu\text{g O}_2 \text{ h}^{-1} [\mu\text{g O}_2 \text{ ml}^{-1}]^{-1}$) is the O_2 conductance of the egg membrane [11].

Equation (2.3) is a differential equation that governs how the internal O_2 concentration, and consequently the realized metabolic rate, B , depend on both intrinsic demand and O_2

supply in the environment. In well-mixed environments without O_2 depletion ($dC_s/dt = 0$), equation 3 can be solved for the equilibrium C_i , which determines the realized metabolic rate, B (equation (2.2)). Using this relationship, we can predict the degree of O_2 limitation for any combination of O_2 supply and demand conditions, where the degree of O_2 limitation is defined as the fraction of intrinsic metabolic demands not met:

$$O_{\text{lim}} = 1 - \frac{B}{D}. \quad (2.5)$$

The parameters of this model were determined by fitting the model to time series of O_2 concentration in closed-system respirometry trials where the change in O_2 concentration within the respirometry chamber, C_o , is

$$\frac{dC_o}{dt} = \frac{-I}{V_o}, \quad (2.6)$$

where V_o is the volume of the respirometry chamber (see the electronic supplementary material, appendix A1). Importantly, water within the respirometry chambers was well mixed during trials such that $C_s \approx C_o$.

(b) Model results

The biophysical model of O_2 supply and demand was able to explain the observed metabolic rate of embryos across a range of temperatures, developmental states and external O_2 concentrations, explaining over 81% of the variation in metabolic rates in all trials. The majority of unexplained variation was due to variation among replicates within a treatment, with the model explaining over 93% of the variation in the mean metabolic rate of eggs across replicate egg (figure 1*b*). The model captured two salient features in the respirometry dataset. First, it predicted that the metabolic rate of embryos in normoxia was largely independent of O_2 when demand was low, but O_2 limited when metabolic demand was high (figure 1*b*, see slopes at O_2 saturation). Second, it predicted that metabolic rate increased with demand when demand was low but plateaued at high demands (figure 1*c* inset). Both patterns emerge from a simple mechanism: as the metabolic rate of embryos increases either due to growth or warming water, their metabolism transitions from being primarily demand driven to supply constrained (figure 1*d*).

Together, these results suggest late-stage developing Chinook salmon embryos are routinely O_2 limited, even at temperatures as low as 8°C in normoxia. The half-saturation constant estimated from the data ($1.47 \mu\text{g O}_2 \text{ ml}^{-1}$; 95% CI: 1.11–1.95) implies that a small degree of O_2 limitation occurs even when C_i is nearly saturated (figure 1*e*). However, severe O_2 limitation occurs for later developmental stages, even in normoxic conditions. For example, in the late stages of development (e.g. 35 days post fertilization [dpf]), the estimated metabolic demand of Chinook salmon embryos at 12°C is roughly $30 \mu\text{g O}_2 \text{ h}^{-1}$, while the realized metabolic rate of these embryos in normoxia was only half this rate (figure 1*c*). Embryos developing in warmer temperatures, or in hypoxic conditions, would experience even more severe O_2 limitation.

(c) Does O_2 limitation explain the thermal tolerance of embryos?

We tested the ability of this model to predict the survival of developing embryos across a range of temperatures where both O_2

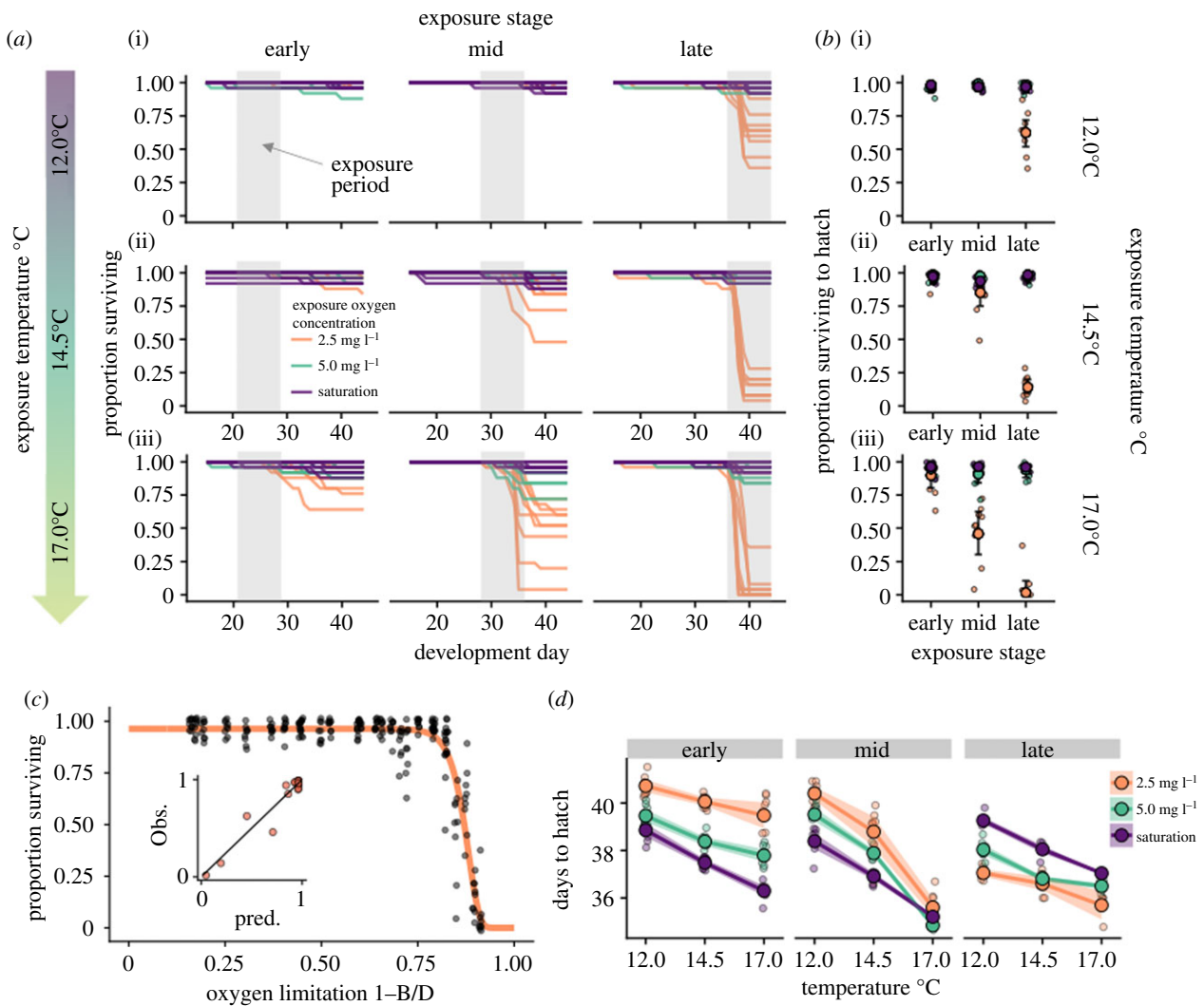


Figure 2. The balance of O₂ supply and demand drives temperature-dependent survival of salmon eggs. (a) Time series of proportion of eggs surviving in nine replicate groups of salmon eggs exposed to one of nine combinations of temperature and dissolved O₂ levels for one week at three different developmental stages. Before and after exposure, eggs were reared at 12°C in normoxic conditions. (b) The proportion of eggs surviving to hatch across treatments depended on the interaction among O₂, temperature and the developmental stage at exposure. Small circles represent the proportion surviving in individual replicates (nine replicates per treatment, 25 eggs per replicate), large circles and error bars show treatment means and 95% confidence intervals. (c) Variation in survival across all combinations of temperature, O₂ and developmental stage at exposure was largely explained by the degree of O₂ limitation (1 - B/D), where B is the realized metabolic rate and D is the intrinsic metabolic demand in the absence of O₂ limitation. Black circles (n = 243) denote values for replicate experimental units from all 27 treatments, circles are slightly jittered. Fitted line shows predicted survival, \hat{S} , where $\hat{S} = S_B e^{-h(0_{lim})}$, where S_B is the background survival probability, and h is the O₂ limitation-dependent hazard rate, which was assumed to be $h = e^{\epsilon_0 + \epsilon_1 0_{lim}}$. Inset shows predicted versus observed mean survival for all 27 treatments. (d) Embryos exposed to hypoxic conditions early in development hatched later than eggs reared in normoxic conditions, while later in development, exposure to hypoxic conditions resulted in early hatching compared to normoxic treatments. (Online version in colour.)

supply and demand were experimentally manipulated. To do this, we exposed eggs at different stages of development to a range of ambient O₂ concentrations and water temperatures for one week and monitored their survival during and after exposure until hatching. Before and after exposure, eggs were reared at the lowest experimental temperature (12°C) in normoxia.

Our experiments revealed that the thermal tolerance of salmon embryos was not fixed but instead depended on development stage and ambient O₂ concentration (figure 2a). In agreement with theoretical predictions, the thermal tolerance of embryos decreased both with elevated O₂ demand associated with later developmental stages, and with decreasing O₂ supply due to reduced ambient O₂ (figure 2a). Moreover, we found an interaction between these two factors: when O₂ demand was low early in development, we observed high survival rates even at low levels of O₂ supply (figure 2b), conversely, when O₂ supply was high, we observed high

survival rates across all exposure temperatures even during the later stages of development when O₂ demand was high.

Evaluating the relationship between O₂ limitation and survival across all treatments revealed that the degree of O₂ limitation was a strong predictor of survival (figure 2c). Interestingly, salmon embryos were able to survive a week-long exposure to O₂ limitation as high as 80% without a substantial reduction in survival. However beyond this level, survival plummeted with further O₂ limitation, with nearly complete mortality above 90% O₂ limitation. Salmon embryos may be able to survive such periods by adaptively slowing their rate of development in response to O₂ limitation. We found that exposure to O₂ limitation early in development could substantially delay the timing of hatching. For example, embryos exposed to the 2.5 µg O₂ ml⁻¹ treatment for just one week, delayed hatching by approximately 2–4 days compared with eggs in normoxic conditions, with

larger delays occurring at warmer temperatures, where the degree of O₂ limitation was more severe (figure 2*d*). Conversely, embryos exposed to hypoxia late in development hatched earlier than eggs in normoxia, suggesting that after a sufficient level of development is reached, O₂ limitation may trigger premature hatching, releasing embryos from the diffusion-constrained O₂ supply within the egg.

(d) Predicting thermal tolerance in natural contexts

Equipped with a mechanistic understanding of the drivers of thermal tolerance, we can begin to understand how salmon eggs are impacted by elevated temperatures in their natural environments. In general, it is thought that temperature is *not* an important driver of survival in natural salmon populations based on the observation that salmon embryos are rarely exposed to temperatures that exceed the laboratory-derived 'lethal' values across their distribution [11]. Importantly, however, this conclusion is based on laboratory experiments conducted in normoxia, whereas our biophysical model predicts that thermal tolerance is substantially reduced in the face of limited O₂ supply. Limited O₂ supply may be especially common for salmon eggs in their natural rearing habitats where adult females release clusters of eggs within a gravel nest or 'redd' in the bed of rivers and streams [12]. The low flows observed in these habitats (typically less than 0.1 cm s⁻¹ [13–15]) allow for significant O₂ depletion to occur, both as water flows through the cluster of eggs, and also within a thin velocity boundary layer that forms around individual eggs [8,16]. To understand how these flow conditions affect the thermal tolerance of salmon eggs in natural contexts, we developed a computational fluid dynamics (CFD) model to simulate O₂ dynamics within a cluster of eggs across a range of flow velocities and temperatures (see the electronic supplementary material, appendix A1). We focused our simulation analysis on the period right before hatching (36 dpf) when the O₂ demand of embryos was the greatest, as this is probably the most critical period for egg survival.

A striking result from the CFD simulations is that embryos within the same cluster of eggs can experience remarkably different local O₂ conditions (figure 3*b*). This heterogeneity emerges from three main sources. First, as water flows through the egg cluster, it gradually becomes depleted of O₂, such that eggs in the downstream half of the cluster experience lower O₂ (figure 3*b*). An additional source of O₂ variation stems from the heterogeneous flow patterns that emerge from the random packing configuration of eggs within cluster (figure 3*a*). This variability in local flow conditions, when coupled with the high metabolic rate of embryos generates variable local O₂ conditions (figure 3*b*). Finally, because of the velocity boundary layer that forms around individual eggs, O₂ concentrations at the surface of the egg are substantially lower than ambient O₂ concentrations. We experimentally tested the presence of local variability in O₂ conditions by measuring fine-scale O₂ distribution within replicate experimental clusters of salmon eggs embedded within gravel-filled PVC pipes (figure 3*c*). In agreement with predictions, we observed high intra-cluster variability in O₂ (SD = 2.7 µg O₂ ml⁻¹). Moreover, this variability was apparent even at the smallest spatial resolution measured (approx. 1 cm, figure 3*c*); O₂ concentrations measured by probes located only a centimetre apart could span the entire range of physically plausible values, from near saturation to near-complete depletion.

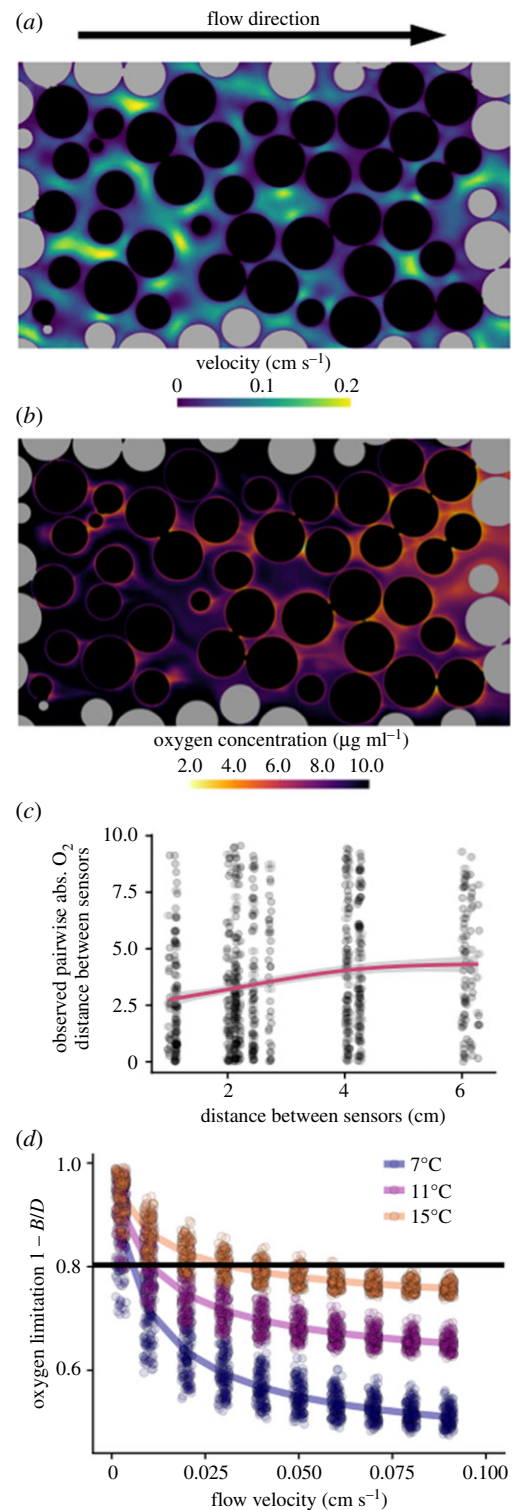


Figure 3. Heterogeneous O₂ dynamics emerge in egg clusters. (a) Representative cross section of flow velocity from a CFD simulation (flow = 0.04 cm s⁻¹, T = 15°C) mimicking the natural rearing environment of salmon eggs. The black and grey circles are egg and gravel cross-sections, respectively. The random packing configuration of eggs and gravel resulted in highly variable flow conditions within the egg cluster. (b) This variability in flow in turn led to highly variable local O₂ conditions, where slow-flowing regions were more heavily depleted of O₂. Additionally, O₂ was depleted as it flowed from the front to the back of the egg cluster. (c) Measured O₂ concentrations within experimental egg clusters were highly variable even at spatial scales as small as 1 cm. Shown are absolute differences in O₂ concentrations between paired O₂ probes within the same egg pocket as a function of the distance between probes. (d) The degree of O₂ limitation for eggs within the cluster in the CFD model depended on flow and temperature. Each point represents one egg within the cluster, lines show the mean O₂ limitation of eggs within a treatment. The black horizontal line represents a critical O₂ limitation, above which mortality increases rapidly with further O₂ limitation (figure 2*c*). (Online version in colour.)

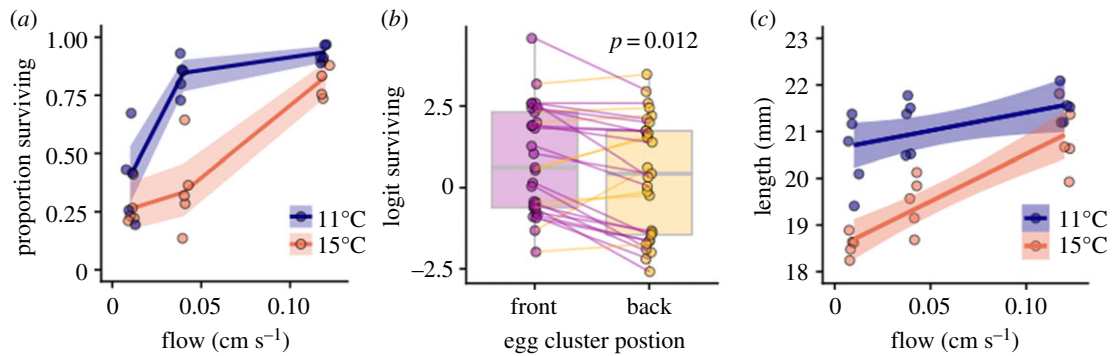


Figure 4. Thermal tolerance in egg clusters. (a) The thermal tolerance of salmon embryos developing in conditions matching their natural habitat—clusters of 200 eggs buried in gravel PVC pipes—was substantially reduced at flow velocities typically observed in natural redds (less than 0.1 cm s^{-1} [13–15]). Shown are the proportion of surviving Chinook embryos reared from fertilization to hatch in five replicate experimental units as a function of experimental temperature and flow velocity. Lines and bands denote the means and 95% CI at each of the 6 treatments. (b) Within experimental replicates, survival was lower in the downstream or back half of the egg cluster, likely due to O_2 depletion as water flows through the egg cluster (figure 3b). Paired points represent logit-transformed proportion survival in each experimental replicate. (c) Flow and temperature conditions in this experiment also affected the mean size at hatch, with embryos hatching at smaller sizes in warmer slower flowing water. (Online version in colour.)

A second major result from the CFD model was that the degree of O_2 limitation experienced by embryos within an egg cluster depends on a nonlinear interaction between temperature and intragravel flow. At high flow velocities, embryos in temperatures as warm as 15°C generally did not experience severe O_2 limitation (figure 3d). However, with decreasing flow velocity, embryos within the egg cluster experienced mortality-inducing O_2 limitation at increasingly lower temperatures. These results suggest that developing salmon eggs in their natural habitat—buried in gravel nests at low flow velocities—will be more sensitive to elevated temperatures than expected based on laboratory studies in normoxia. To test this prediction, we conducted an additional experiment, where we buried clusters of 200 eggs within gravel-filled PVC pipes, and experimentally manipulated flow and temperature. As predicted by the CFD model, the thermal tolerance of eggs in these experiments was strongly dependent on flow (figure 4a). At high flow velocity (0.12 cm s^{-1}), survival was high across both experimental temperatures (11 and 15°C). However, at the lower flow velocities (less than 0.1 cm s^{-1}) more representative of the natural condition in redds [13–15], we observed substantial temperature-dependent mortality. At an intermediate flow velocity, the onset of temperature-dependent mortality occurred at 15°C , while at the lowest flow velocity, we observed elevated mortality even at our lowest experimental temperature, 11°C . As further evidence of O_2 -dependent survival, we found eggs located in the downstream, more O_2 deprived half of the egg cluster (figure 3b), survived at lower rates than eggs in the front of the egg pocket (paired *t*-test $p = 0.012$; figure 4b).

In addition to lethal effects, O_2 limitation also impacted the size of hatched embryos in ways that largely mirrored patterns in survival, with embryos hatching at smaller sizes in warmer and slow-flowing water (figure 4c). This provides further evidence that O_2 limitation drives embryos to escape the egg capsule earlier in development.

3. Discussion

Our results provide strong theoretical and empirical support for the hypothesis that the decreased thermal tolerance of fish embryos, relative to other life stages, is due to constraints on

O_2 supply within the egg [8]. As predicted by our O_2 limitation hypothesis, the thermal tolerance of embryos decreased with increasing demand associated with development, and with reductions in O_2 supply, either due to ambient O_2 concentration or environmental flow. Moreover, thermal tolerance across all of these conditions could be predicted from a simple biophysical model of O_2 supply and demand. This insight into the mechanistic basis of thermal tolerance of fish eggs has important implications for predicting how fish populations will respond to climate change.

Across experimental conditions, the thermal tolerance of Chinook embryos varied by as much as 6°C . This context dependency of thermal tolerance observed in our study and others [8,17,18] poses a challenge for predicting how species will respond to climate change. For example, we found that thermal tolerance of embryos depends on complex, nonlinear interactions between developmental stage, ambient O_2 concentration, flow velocity and the presence of neighbouring eggs. To assess the effects of all of these factors and their interactions empirically would quickly result in a combinatorial explosion infeasible for all but the best-studied species. Importantly however, a mechanistic understanding of thermal tolerance compresses the problem to manageable dimensions. Rather than having to fit a unique thermal performance curve for each combination of relevant variables, knowledge of the mechanisms underlying thermal tolerance allows us to make *a priori* predictions of how novel conditions will shift thermal tolerance. In the case of salmon embryos, thermal tolerance is set by the balance between temperature-dependent O_2 demand and diffusion-limited supply. This allowed us to predict how the thermal tolerance of Chinook salmon embryos would shift in natural contexts, where O_2 supply is limited due to low environmental flows. Not only were these predictions confirmed experimentally, they also explain the recent near-complete cohort loss of an endangered Chinook salmon population that occurred over several drought years where water temperatures were 3°C lower than the lethal levels predicted from laboratory experiments [8]. More broadly, this mechanistic understanding will be critical for predicting how species will respond to aquatic environments that are simultaneously warming and losing O_2 [19].

A longstanding goal of ecophysiology is to understand and predict interspecific variation in thermal tolerance [20–22].

The biophysical model developed here provides a mechanistic framework for making such predictions. Across species, the metabolic rate of embryos is proportional to egg volume [8], but supply occurs by diffusion across the egg surface [6]. Thus, larger eggs should become O₂ limited at lower temperatures, and as a result our theory predicts that thermal tolerance should decrease with egg size. This prediction is supported by global patterns of fish egg sizes, where mean egg diameter is negatively correlated with sea surface temperature [23]. Moreover, for eggs of similar sizes, our theory makes testable predictions on how thermal tolerance should vary with species traits (e.g. volume-specific metabolic rate, surface-area-specific O₂ conductance) that can be measured from standard respirometry assays.

The differential scaling of O₂ supply and demand with egg volume sets fundamental constraints on egg size in aquatic systems. The predominant trend in aquatic systems is that adults produce offspring in proportion to their size [24]. Specifically, in aquatic organisms ranging in mass over 17 orders of magnitude, adults of most species produce offspring that on the order of one-hundredth their mass. Teleosts, however, are a striking exception to this pattern, as offspring size is independent of adult body size [24]. Our results suggest this pattern emerges because these eggs approach sizes where O₂ limitation constrains offspring size. Although elasmobranchs and marine mammals are as large or larger than teleosts and produce large offspring in proportion to their body size, in both cases, these taxa have evolved physiological adaptations to overcome the limitations of diffusion across an egg surface. For example, marine mammals supply O₂ to developing embryos through the placenta, and embryos of oviparous elasmobranchs are able to generate flow through slits that form in the egg case [25]. Because teleosts have not evolved similar adaptations, they are constrained to produce more offspring instead of larger offspring. As a result, teleosts are among the most fecund animals on the planet, with profound implications for their life history and demography [26].

In summary, our biophysical model of O₂ limitation accurately predicted the thermal tolerance of Chinook salmon eggs across a range of organismal and environmental conditions. Moreover, O₂ limitation explains the elevated sensitivity of fish eggs relative to other life stages [5], global patterns in fish egg size [23] and the extreme fecundity of large teleosts [24]. As eggs are one of the most thermally sensitive life stages in fishes [5], the mechanistic understanding developed here will be critical for predicting how fishes respond to a warming climate.

4. Methods

(a) Survival experiments

Approximately 8000 freshly fertilized Chinook salmon eggs from six female × male crosses were collected from Coleman National Fish Hatchery and transported in aerated coolers to NOAA's Fisheries Ecology Division of the Southwest Fisheries Science Center (SWFSC, Santa Cruz, CA). Upon arrival eggs from all females were well mixed into a common pool. From this pool groups of 25 eggs were placed into one of 243 individual 50 mm diameter aquaponic baskets and assigned to one of 27 treatments (nine replicates per treatment). Additional baskets of eggs were set aside for respirometry trials. The baskets were then placed into a Heath (Flex-a-lite Consolidated) recirculating incubation tray, where water temperatures were maintained at

12°C. Water was recirculated through the Heath tray at a flow rate of 19 l min⁻¹, and slits in the sides of baskets allowed water to flow through the baskets and over the eggs. Water quality was maintained using an inline ultraviolet light sterilizer and daily approximately 25% water changes.

Post-transfer, eggs were left to acclimate for a period of two weeks prior to the collection of mortality data. During this time, any dead eggs in the baskets were replaced with surplus eggs reared at the same temperature. Temperature and O₂ in the Heath tray were measured twice daily, with temperatures maintained between 11.9°C and 12.6°C, and O₂ never fell below 9.38 µg O₂ ml⁻¹.

At three different developmental stages (21, 28, 35 dpf), groups of eggs (9 replicate baskets per treatment) were moved to one of nine experimental aquaria (12 l; electronic supplementary material, figure S3). Each experimental tank was kept at one of three temperatures (12, 14.5, 17°C) and three O₂ levels (saturation, 5.0 and 2.5 µg ml⁻¹). Experimental tanks were held in circulating water baths heated with submersible heaters and temperature was maintained through thermostat controllers placed within the experimental tanks.

O₂ levels were maintained by bubbling nitrogen (N₂) gas to strip O₂ from the water in 500 L reservoirs. O₂ levels were monitored using Loligo systems optical O₂ probes and nitrogen delivery was controlled by the program WitroxView via solenoid valves. Water was pumped from the reservoirs to each experimental tank at a rate of 5 ml s⁻¹ and O₂ and temperature levels in the experimental tanks were monitored via a YSI ProODO optical handheld O₂ metre three times daily. Additionally, a mini recirculation pump was placed in each tank to generate a circulating flow in the circular tanks to prevent local O₂ depletion around the eggs. Eggs were kept in these conditions for one week, and then moved back to the 12°C, normoxic conditions in the Heath tray. Before, during and after exposure, eggs were monitored daily for mortality, and any dead eggs were removed from the baskets.

(b) Respirometry

We conducted closed-system respirometry experiments to measure the metabolic rate of developing Chinook embryos as a function of developmental state (dpf) and temperature. Starting from 15 dpf, we ran respirometry trials for each of the three temperature treatments, once per week, for four weeks. In addition, we conducted three trials at 8°C to cover a larger range of temperatures and generate a more robust estimate of the temperature dependence of metabolic rate.

Before the respirometry trials, all eggs were reared at 12°C in normoxic conditions and brought up to the experimental temperature over 30 min before each trial. Experiments were conducted using a Loligo Systems microplate, with 24 1.7 ml wells. Each well was equipped with an O₂ sensor spot (PreSens) to measure O₂ within the chamber. Experimental temperatures were maintained by placing the microplate system in a flow through a bath, connected to a high-precision temperature control system (Thermo-fisher SC100 controller paired with A28F bath circulator). To ensure water within the respirometry chambers was well mixed, we placed 6 mm glass-coated magnetic spin bars (Loligo Systems) into each of the 24 wells and placed the entire microplate system on a magnetic stir plate. To avoid disturbance of the eggs by the spin bars, we inserted thin stainless steel mesh screens approximately 6 mm above the bottom of the well. This allowed enough room below the screen for the bars to spin and enough room above the screen for the eggs to fit into the wells. For each trial, 12–16 eggs were placed in randomly selected chambers, with the remaining wells serving as blanks. The microplate system was sanitized with a diluted bleach solution between each trial. After sealing the microplate with a layer of parafilm and a soft-silicone

gasket, we began recording O_2 at 4 s intervals. We continued to record O_2 in each well until O_2 within each well containing an egg had dropped to below 10% of saturation. During the experiments, the wells were visually inspected to ensure the magnetic bars were spinning in each well. Any well with a bar that stopped spinning was excluded from analysis.

(c) O_2 distribution in simulated egg clusters

An experiment to measure the variability of O_2 within an egg cluster was conducted at Coleman National Fish Hatchery (Anderson, CA). To simulate the environment within a redd, we assembled 'egg clusters' within six, 15 cm diameter PVC pipe sections. The PVC pipe was capped and screened at the bottom and gravel was filled to a base depth of approximately 30 cm. Each egg tube received a 25:75 mixture of 1.90 and 2.54 cm grade gravel. To create an egg pocket, a 5 cm diameter sleeve was placed in the centre of the PVC pipe on top of the base fill and gravel was filled in around it to a depth of approximately 7 cm. Once all O_2 probes were inserted (see below) approximately 1000 *O. mykiss* eggs (at approximately 260 degree days of development; Troutlodge Sumner, Washington) were poured through the 5 cm PVC pipe into the pocket and then the PVC pipe was removed. The egg pocket was then carefully capped with approximately 15 cm of the same gravel. For the experiment, we used two temperature treatments (11 and 15°C, 3 replicates per temperature) at an intermediate flow velocity (0.04 cm s⁻¹).

Sixteen *in situ* O_2 probes were inserted into each of the egg pocket cylinders (electronic supplementary material, figure S3). The probes were arranged at four levels within the egg pocket (1, 3, 5 and 7 cm elevation from the base of the egg pocket) with four probes per level placed radially at 0, 90, 180 and 270 degrees from a vertical index (see electronic supplementary material, figure S4 for a detailed diagram of probe locations).

The O_2 probes and measurement system were assembled in-house. The core of the O_2 measurement system is the sensor spots and optical spectrometer (PreSens Precision Sensing GmbH, Regensburg, Germany). The 3 mm diameter sensor spots that fluoresce when light (505 nm) is shone upon them were glued, using optical epoxy, onto the distal ends of 96 fibre optic cables, which were sheathed in stainless steel tubing (4 mm diameter × 15 cm length). Because of their small diameter, the O_2 probes are minimally disruptive to the flow through the redd. The fibre optic cable probes were connected to a custom optical multiplexer (Agiltron Inc., Woburn MA, USA), which was in turn connected to the optical spectrometer. The system gathered an O_2 reading every one second while the script cycled the optical multiplexer through the 96 fibre optic channels on an approximately 20 s interval. One complete cycle took about 35 min. The cycle was repeated continuously for the duration of the experiment (approx. 6 h).

(d) Survival in simulated egg clusters

An experiment to measure the effect of the flow velocity on thermal tolerance in conditions matching those of natural salmon nests was conducted at Coleman National Fish Hatchery. In this experiment, groups of 200, 1-day post-fertilization Fall-run Chinook eggs from Coleman Hatchery were placed within a gravel upweller tube at one of two constant temperatures (11 and 15°C) and one of three flow rates (0.01, 0.04, and 0.12 cm s⁻¹). Each temperature system consisted of an aerated head tank that gravity fed constant temperature water to 15 tubes (five tubes per flow rate). Water height in each

tube was set 5 cm above the outlet by an external standpipe while upwelling flow was controlled by specific valves (Parker Hannifin brass ¼ inch (0.01 cm s⁻¹) and ⅜ inch valves (0.04 cm s⁻¹), and Marquest Scientific PVC ½ inch needle valve (0.12 cm s⁻¹). Based on our CFD analysis, we hypothesized that eggs in that back half of the egg cluster would experience lower survival due to O_2 depletion. We tested this hypothesis by separating the egg pocket into two mesh bags (2 mm mesh), which allowed water to flow freely through the bag, but kept the eggs and hatched alevins enclosed. The first mesh bag was placed on gravel 15 cm above the tube inlet, and the second bag was placed above (downstream) of the first bag. Seventy-six centimetres of gravel covered the second bag to complete the upweller artificial redd. Velocity ($v = 0.01, 0.04, \text{ or } 0.12 \text{ cm s}^{-1}$) was randomly assigned to the five replicate tubes within each temperature array of 15 tubes and target flow rate ($Q = \text{cm}^3 \text{ s}^{-1}$) was calculated as, $Q = v P A$, where P is the porosity of the gravel in the PVC pipe (measured before the experiment), and A is the cross-sectional area of the PVC pipe. Target flow was checked every other day with a graduate cylinder (ml in 30 s) and temperature recorded hourly with an Onset temperature probe (Onset, Bourne MA).

A separate group of eggs was incubated at each experimental temperature within a Heath tray for assessment of egg viability and time of hatch. Tubes were sampled after 33 (15°C) and 48 days (11°C) when the cohort Heath tray eggs were hatched. Dead eggs and alevins were counted in each mesh bag replicate. Viable alevins were then euthanized by an overdose of MS222 and measured for length (0.01 mm caliper).

(e) Statistical analyses

Statistical analysis of survival was conducted using a generalized linear mixed model in R [27,28], with a binomial error and a logit link function. Experimental units (replicate baskets or tubes) were treated as a random variable. Because of the expected non-linear relationship between survival and independent variables, we treated independent variables as discrete factors rather continuous variables.

Ethics. The experiments conducted at Southwest Fisheries Science Center were approved by the University of California Santa Cruz Animal Care and Use Committee (IACUC no. Kierj1904). The experiments at Coleman Fish Hatchery were conducted with the permission of the Coleman National Fish Hatchery management and followed the recommendations put forth in guidelines for the use of fisheries in research (2014).

Data accessibility. All data and code to run the analyses are provided can be downloaded at GitHub: <https://github.com/btmarti25/biophysical-basis-of-thermal-tolerance-in-aquatic-eggs>.

Authors' contributions. B.T.M. conceived the study, developed the biophysical model, analysed the data and wrote the manuscript. P.N.D. developed and analysed the CFD model. B.T.M., N.S.K., D.M.S., W.J.R., D.T., A.M.D.R., J.S.F. and E.M.D. designed the experiments, and B.T.M., N.S.K., D.M.S., W.J.R., D.T. and J.S.F. performed the experiments. All authors contributed revisions of the manuscript.

Competing interests. We declare we have no competing interests.

Funding. This study was supported by California State Water Resources Control Board (grant no. 19-028-300).

Acknowledgements. The authors thank Andrew Hein for comments and suggestions on an earlier version of the manuscript. We thank Kristin Saksa, Hayley Mapes and Ron Stone for assistance with performing the experiments.

References

- Pörtner HO, Bock C, Mark FC. 2017 Oxygen-and capacity-limited thermal tolerance: bridging ecology and physiology. *J. Exp. Biol.* **220**, 2685–2696. (doi:10.1242/jeb.134585)
- McCullough DA. 1999 *A review and synthesis of effects of alterations to the water temperature*

- regime on freshwater life stages of salmonids, with special reference to Chinook salmon. Seattle, WA: US Environmental Protection Agency.
3. Eliason EJ, Clark TD, Hague MJ, Hanson LM, Gallagher ZS, Jeffries KM, Farrell AP. 2011 Differences in thermal tolerance among sockeye salmon populations. *Science* **332**, 109–112. (doi:10.1126/science.1199158)
 4. Whitney CK, Hinch SG, Patterson DA. 2013 Provenance matters: thermal reaction norms for embryo survival among sockeye salmon *Oncorhynchus nerka* populations. *J. Fish Biol.* **82**, 1159–1176. (doi:10.1111/jfb.12055)
 5. Dahlke FT, Wohlrab S, Butzin M, Pörtner HO. 2020 Thermal bottlenecks in the life cycle define climate vulnerability of fish. *Science* **369**, 65–70. (doi:10.1126/science.aaz3658)
 6. Kranenborg S, Muller M, Gielen JLW, Verhagen JHG. 2000 Physical constraints on body size in teleost embryos. *J. Theor. Biol.* **204**, 113–133. (doi:10.1006/jtbi.2000.1093)
 7. de Salvo Souza R, Soncini R, Glass M, Sanches J, Rantin F. 2001 Ventilation, gill perfusion and blood gases in dourado, *Salminus maxillosus* Valenciennes (Teleostei, Characidae), exposed to graded hypoxia. *J. Comp. Physiol. B* **171**, 483–489. (doi:10.1007/s003600100198)
 8. Martin BT, Pike A, John SN, Hamda N, Roberts J, Lindley ST, Danner EM. 2017 Phenomenological vs. biophysical models of thermal stress in aquatic eggs. *Ecol. Lett.* **20**, 50–59. (doi:10.1111/ele.12705)
 9. Marshall DJ, Pettersen AK, Bode M, White CR. 2020 Developmental cost theory predicts thermal environment and vulnerability to global warming. *Nat. Ecol. Evol.* **4**, 406–411. (doi:10.1038/s41559-020-1114-9)
 10. Rombough PJ. 1994 Energy partitioning during fish development: additive or compensatory allocation of energy to support growth? *Funct. Ecol.* **8**, 178–186. (doi:10.2307/2389901)
 11. Quinn TP. 2018 *The behavior and ecology of pacific salmon and trout*. Seattle, WA: University of Washington Press.
 12. Hawke SP. 1978 Stranded redds of quinnat salmon in the Mathias River, South Island, New Zealand. *New Zealand J. Mar. Freshwater Res.* **12**, 167–171. (doi:10.1080/00288330.1978.9515737)
 13. Zimmermann AE, Lapointe M. 2005 Intergranular flow velocity through salmonid redds: sensitivity to fines infiltration from low intensity sediment transport events. *River Res. appl.* **21**, 865–881. (doi:10.1002/rra.856)
 14. Malcolm IA, Youngson AF, Soulsby C, Imholt C, Fryer RJ. 2011 Is interstitial velocity a good predictor of salmonid embryo survival? *Trans. Am. Fish Soc.* **140**, 898–904. (doi:10.1080/00028487.2011.601216)
 15. Sear DA, Pattison I, Collins AL, Newson MD, Jones JJ, Naden PS, Carling PA. 2014 Factors controlling the temporal variability in dissolved oxygen regime of salmon spawning gravels. *Hydrol. Processes* **28**, 86–103. (doi:10.1002/hyp.9565)
 16. Daykin PN. 1965 Application of mass transfer theory to the problem of respiration of fish eggs. *J. Fish. Board Can.* **22**, 159–171. (doi:10.1139/f65-014)
 17. Del Rio AM, Davis BE, Fangue NA, Todgham AE. 2019 Combined effects of warming and hypoxia on early life stage Chinook salmon physiology and development. *Conserv. physiol.* **7**, coy078. (doi:10.1093/conphys/coy078)
 18. Giomi F, Barausse A, Duarte CM, Booth J, Agusti S, Saderne V, Fusi M. 2019 Oxygen supersaturation protects coastal marine fauna from ocean warming. *Sci. adv.* **5**, eaax1814. (doi:10.1126/sciadv.aax1814)
 19. Breitburg D, Levin LA, Oschlies A, Grégoire M, Chavez FP, Conley DJ, Jacinto GS. 2018 Declining oxygen in the global ocean and coastal waters. *Science* **359**, aam7240. (doi:10.1126/science.aam7240)
 20. Leiva FP, Calosi P, Verberk WC. 2019 Scaling of thermal tolerance with body mass and genome size in ectotherms: a comparison between water-and air-breathers. *Phil. Trans. R. Soc. B* **374**, 20190035. (doi:10.1098/rstb.2019.0035)
 21. Sunday J, Bennett JM, Calosi P, Clusella-Trullas S, Gravel S, Hargreaves AL, Morales-Castilla I. 2019 Thermal tolerance patterns across latitude and elevation. *Phil. Trans. R. Soc. B* **374**, 20190036. (doi:10.1098/rstb.2019.0036)
 22. Stillman JH, Somero GN. 2000 A comparative analysis of the upper thermal tolerance limits of eastern Pacific porcelain crabs, genus *Petrolisthes*: influences of latitude, vertical zonation, acclimation, and phylogeny. *Physiol. Biochem. Zool.* **73**, 200–208. (doi:10.1086/316738)
 23. Barneche DR, Burgess SC, Marshall DJ. 2018 Global environmental drivers of marine fish egg size. *Glob. Ecol. Biogeogr.* **27**, 890–898. (doi:10.1111/geb.12748)
 24. Neuheimer AB, Hartvig M, Heuschele J, Hylander S, Kjørboe T, Olsson KH, Andersen KH. 2015 Adult and offspring size in the ocean over 17 orders of magnitude follows two life history strategies. *Ecology* **96**, 3303–3311. (doi:10.1890/14-2491.1)
 25. Musa SM, Czachur MV, Shiels HA. 2018 Oviparous elasmobranch development inside the egg case in 7 key stages. *PLoS ONE* **13**, e0206984.
 26. Streelman T, Puchulutegui J, Bass C, Thys AL, Dewar T, & Karl H, A S. 2003 Microsatellites from the world's heaviest bony fish, the giant *Mola mola*. *Mol. Ecol. Notes* **3**, 247–249. (doi:10.1046/j.1471-8286.2003.00413.x)
 27. Core Team R. 2018 *R: a language and environment for statistical computing*. Vienna, Austria: R Foundation for Statistical Computing. See <https://www.R-project.org>.
 28. Bates D, Maechler M, Bolker B, Walker S, Christensen RHB, Singmann H, Bolker MB. 2015 Package 'lme4'. *Convergence* **12**, 2.